ACS APPLIED MATERIALS & INTERFACES

Research Article

www.acsami.org

Microbeads and Hollow Microcapsules Obtained by Self-Assembly of Pickering Magneto-Responsive Cellulose Nanocrystals

Tiina Nypelö,*[,†,⊥] Carlos Rodriguez-Abreu,*[,§] Yury V. Kolen'ko,[§] José Rivas,[§] and Orlando J. Rojas[†,‡,∥]

[†]Department of Forest Biomaterials and [‡]Department of Chemical and Biomolecular Engineering, North Carolina State University, Raleigh, North Carolina 27695, United States

[§]International Iberian Nanotechnology Laboratory, Av. Mestre José Veiga, 4715-330 Braga, Portugal

[∥]School of Chemical Technology, Department of Forest Products Technology, Aalto University, 00076 Aalto, Finland

Supporting Information

ABSTRACT: Cellulose microbeads can be used as immobilization supports. We report on the design and preparation of magneto-responsive cellulose microbeads and microcapsules by self-assembled shells of cellulose nanocrystals (CNC) carrying magnetic $CoFe_2O_4$ nanoparticles, that is, a mixture of isotropic and anisotropic nanomaterials. The magnetic CNCs formed a structured layer, a mesh, consisting of CNCs and magnetic particles bound together on the surface of distinct droplets of hexadecane and styrene dispersed in water. Because of the presence of CNCs the highly crystalline mesh was targeted to provide an improved barrier property of the microbead shell compared to neat polymer shells, while the magnetic particles provided the magnetic response. In situ polymerization of the styrene phase led to the formation of solid microbeads (~8 μm diameter) consisting of polystyrene (PS) cores encapsulated in the magnetic CNC shells (shell-to-core mass ratio of 4:96). The obtained solid microbeads were ferromagnetic (saturation magnetization of ~60 emu per gram of the magnetic phase). The magnetic functionality enables easy separation of substances immobilized on the beads. Such a functionality was tested in removal of a dye from water. The microbeads were further utilized to synthesize hollow microcapsules by solubilization of the PS core. The CNC-based, magneto-responsive solid microbeads and hollow microcapsules were characterized by electron microscopy (morphology), X-ray diffraction (phase composition), and magnetometry (magnetic properties). Such hybrid systems can be used in the design of materials and devices for application in colloidal stabilization, concentration, separation, and delivery, among others.

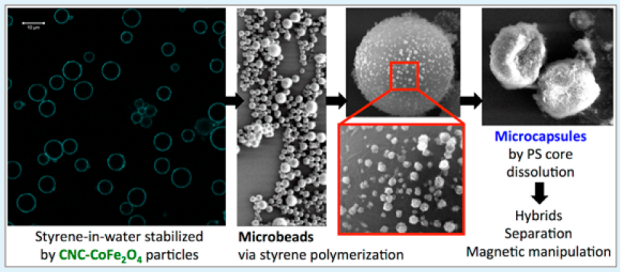

KEYWORDS: *cellulose nanocrystals, microcapsules, magnetic microbeads, Pickering emulsions, scavengers*

INTRODUCTION

Cellulose nanocrystals (CNCs) are shape-anisotropic particles obtained by acid hydrolysis of cellulose fibers or fibrils.[1] CNCs are highly crystalline, rigid, and nontoxic nanoparticles.[2] These properties are appealing in a plethora of materials ranging from composites to medical devices. Recently CNCs have been deployed as emulsion stabilizers[3−8] by taking advantage of their self-assembling ability at the oil/water interface, similarly to particle-stabilized Pickering systems.[9] Because of the high energy required for desorption of the particles from the surface, Pickering emulsions are extremely stable.[10] These emulsions have further been demonstrated as a precursor for microbeads encapsulated by neat CNCs producing cellulose microspheres.[11]

In general, microspheres can be utilized in medical applications[12] as well as in separation of contaminants from wastewaters.[13] Cellulose-coated microspheres and microcapsules have found potential use for controlled release[14] and separation.[15] Traditional polymer microcapsules usually suffer from poor barrier properties of the encapsulating polymer membrane, making it difficult to encapsulate, for example, liquids. Advances on this have been sought in preparing metal-encapsulated microbeads.[16]

Many recent efforts in the field of cellulosic materials have dealt with construction of stimuli-responsive cellulosic nanomaterials for sensing, detection, and separation.[17,18] Such efforts often involve impregnation of responsive particles into a cellulosic matrix to prepare, for example, photoswitchable films[19] and systems with tunable wettability.[20] Magnetic cellulose structures and magnetic paper have been prepared by precipitating magnetite or ferrite particles onto fiber matrices[21−25] or by loading fiber lumens.[26] Some works have utilized cellulose nanofibrils either as a synthesis template[27,28] or as a matrix to embed preformed magnetic particles.[29] In addition to the cellulosic nanofibrils, interest in developing magnetic cellulose nanocrystal material has been vast. Very

Received: July 1, 2014
Accepted: September 15, 2014
Published: September 15, 2014

recently a few works have simultaneously introduced attachment of magnetic particles on CNCs or synthesis of the inorganic particles on CNCs producing material that has been suggested to have potential, for example, in separation applications.[30,31]

Among the many uses for magnetic materials, magneto-responsive Pickering systems have been introduced by Velev et al.[32,33] demonstrating effective stabilization of foams by a mixture of magnetic and nonmagnetic particles. They used magnetic manipulation of the foams stabilized by hypromellose phthalate and iron particles enabling stimuli-responsive non-contact destruction of the foams. Considering the outstanding ability of CNCs to stabilize Pickering emulsions[3] and their proven applicability in separation,[34] CNCs should be utilizable in magneto-responsive Pickering emulsions as well.

Here we present the assembly of magneto-responsive CNC material comprising isotropic and anisotropic nanoparticles[35] at an oil−water interface to prepare magneto-responsive Pickering emulsions as precursor for magnetic solid microbeads and hollow microcapsules. Hence, we expand on the approach to encapsulate oil droplets with a pure CNC shell by providing functionality with in situ-synthesized inorganic magnetic particles. We demonstrate proof-of-concept application of these systems in encapsulation, magnetic concentration, and separation of target molecules.

EXPERIMENTAL SECTION

Preparation of Cellulose Nanocrystals. The CNCs were manufactured by hydrolysis of cotton fibers using 65 wt % sulfuric acid for 30 min as described previously.[1] The hydrolysis was stopped by pouring the dispersion into an ice bath and was then filtered and centrifuged to remove the excess acid. Finally, the CNC dispersion was dialyzed for approximately one week using membranes with molecular weight cutoff of 12−14 kDa. The resulting CNCs were ca. 7 and 150 nm in width and length (Figure S1 in the Supporting Information). CNCs prepared using sulfuric acid hydrolysis carry negative charges through esterification of surface hydroxyl groups during the acid hydrolysis. According to elemental analysis the amount of the sulfate half-ester groups on the surface of CNC was 0.74 wt %, in agreement with previous data on similar materials.[1]

Preparation of CNC−$CoFe_2O_4$ Hybrids. The magneto-responsive CNC material was prepared as described by us previously.[35] In brief, ferrous(II) sulfate heptahydrate (Fluka), cobalt chloride, and potassium nitrate (both from Fisher Scientific) were used as received to synthesize magnetic nanoparticles in the presence of the CNC aqueous dispersion by coprecipitation (2:1 molar ratio). The dispersion was heated to 95 °C and kept for 3 h followed by sonication. The resulting dispersion was centrifuged, and the supernatant was replaced with Milli-Q-water. Sodium hydroxide (0.33 M final concentration) and potassium nitrate (0.03 M final concentration) were then added to the mixture. After alkaline addition, the mixture was sonicated and stirred at ca. 90 °C for 1 h. The resulting dispersion was again centrifuged; the supernatant was replaced with Milli-Q-water, redispersed, and finally dialyzed for 3 d using membranes with molecular weight cutoff of 12−14 kDa. This led to a homogeneous dispersion of magnetic CNC−$CoFe_2O_4$ hybrids. This dispersion was placed next to a NdFeB magnet to recover by magnetic attraction only strongly coupled CNC−$CoFe_2O_4$ particles, which were later used for emulsification.

Preparation of Microbeads Encapsulated in CNC Shells. For emulsification and stabilization of oil/water interface with CNCs we used established methods.[3,4] In a typical experiment, a 10 mg mL^{-1} aqueous suspension of CNC−$CoFe_2O_4$ was sonicated for 20 s using a Branson (model 250) tip sonicator. A total of 0.25 mL of oil phase was added to 1 mL of the aqueous CNC−cobalt ferrite suspension, and an emulsion was produced upon sonication for 20 s (3 s pulse, alternating with 3 s pulse off). The ability of CNCs to assemble at the interface of oil-in-water emulsions was demonstrated using hexadecane/water (30/70 by weight) systems that were sonicated in the presence of 0.8 wt % CNC. Approximately 7 mM NaCl was added to the aqueous CNC dispersion prior to hexadecane-in-water emulsion formation. In some experiments CNC and CNC−$CoFe_2O_4$ dispersions were dyed with Calcofluor white stain (Fluka) prior to emulsion preparation. To prepare solid microbeads carrying CNC shells styrene was mixed with an initiator (2,2′-azobis(2,4-dimethyl)valeronitrile) (100:3 mass ratio), and similarly the monomer-initiator mixture was added to CNC−cobalt ferrite suspension (0.25 to 1 mL, respectively) and sonicated. Then, the emulsions were diluted by adding 0.5 mL of water with vortex-mixing; the styrene polymerized under agitation in a dry bath at 70 °C for 24 h. Following this, the obtained hybrid polystyrene (PS)-based particles were separated with a NdFeB magnet, and the supernatant was discarded. The recovered particles were dried under vacuum at room temperature.

Material Characterization. Oil-in-water emulsions were observed using a confocal fluorescence microscope (Zeiss LSM 710 confocal) attached to a Zeiss Axio Observer Z1. Aqueous dispersions of microbeads were observed under a Nikon SMZ-1500 optical microscope using transmitted light. Particle dimensions were determined with ImageJ software. Reported sizes are averages over 400−500 measurements. A Nanoscope IIIa/Dimension 3000 (Bruker) atomic force microscope (AFM) operated with silicon cantilevers in tapping mode was used for imaging CNC dispersions that were spin-coated on silicon substrates.

Microscopic images as well as data on local chemical composition of the cellulosic particles were collected using a Quanta 650 FEG ESEM instrument (FEI Company) fitted with an INCA 350 energy-dispersive X-ray spectrometer (EDS) (Oxford Instruments). Samples were deposited from aqueous dispersions on silicon wafers and then dried under vacuum. Chemical composition of selected samples was estimated by using inductively coupled plasma−optical emission spectrometer (ICP−OES) on a DV2000 spectrometer (PerkinElmer).

Powder X-ray diffraction (XRD) data were collected on an X'Pert PRO diffractometer (PANalytical) set at 45 kV and 40 mA and equipped with Cu Kα radiation (λ = 1.541 874 Å) using Bragg−Brentano geometry in the 20 to 100° 2θ range with a scan speed of 0.006° s^{-1}. The XRD patterns were matched to those in the Crystallography Open Database (COD) using HighScore software package (PANalytical).

The inorganic loading in the materials was determined using thermogravimetric analysis (TGA) on a Mettler-Toledo TGA/DSC 1 STAR^e instrument in N_2 or O_2 atmosphere. For the analysis, samples were heated from 25 to 700 °C (20 °C min^{-1}) and then kept during 5 min at 700 °C. The magnetic properties of the particles at 298 K were measured using a MicroSense EV9 vibrating sample magnetometer (VSM). Measurements of magnetization versus applied magnetic field (from −20 kOe to 20 kOe) were carried out on powder samples obtained by drying the particle dispersions in vacuum. The magnetization values are expressed per mass of magnetic material, estimated from TGA analysis of the dry particles.

Separation from aqueous solution of a cationic dye, methylene blue, was performed as follows: 4 mg of CNC−cobalt ferrite PS microbeads were mixed with 1 mL of methylene blue solution (1 mg L^{-1} and 10 mg L^{-1} concentration). A NdFeB magnet was used to separate the magnetic particles. The liquid was removed and centrifuged at 12 000 rpm for 10 min. The UV−vis spectrum of the supernatant was then measured in a 1 mm path cuvette using a Shimadzu UV-2550 spectrometer. The extent of removal of the dye was determined from the difference in spectral signal before and after particle magnetic concentration and removal.

RESULTS AND DISCUSSION

Our aim was to prepare microbeads enclosed in a magneto-responsive shell consisting of magnetically modified cellulose material to provide functional microbeads via self-assembly. We chose CNCs as the cellulosic constituent due to their ability to self-assemble at oil/water interface in suitable conditions. The

magneto-responsive CNC material for encapsulating oil-in-water emulsions was prepared by synthetizing cobalt ferrite particles in situ from precursor salts as described by us elsewhere.[35] This previously reported approach led to inorganic loading of 7 wt %. We found, however, that, by applying to the dispersions a magnetic field with a NdFeB magnet, $CoFe_2O_4$-loaded CNCs could be separated from the unloaded CNCs, resulting in a final product with a much higher inorganic ($CoFe_2O_4$) content (48 wt % as determined by TGA, included in the Supporting Information, Figure S2). This magnetic separation enabled the recovery of the CNCs loaded with $CoFe_2O_4$ from the neat CNC (approximately 44 wt % of the total). The magnetic fields would have removed selectively the inorganic particles from the dilute dispersion (ca. 1 wt %) if the interaction between the CNC and the magnetic nanoparticles was weak. Hence, the remaining CNCs particles can be deemed to be coupled with the magnetic particles. The synthesis of the CNC hybrid material was done by introducing the precursor salt to a CNC dispersion, thermal precipitation of the salts on CNCs, and particle growth via alkaline addition.[35] Therefore, the interactions between CNC and ferrite nanoparticles probably involve strong interactions between the sulfate groups of CNC and the nanoparticles, for example, via coordination bonding, attraction between electron−poor and electron−rich groups, acid−base interactions, etc. The quality of the magnetic component was confirmed by the XRD profile (Figure 1a) that fitted well the cobalt ferrite reference spectrum.

The inorganic particles were well-dispersed within the CNCs as observed by SEM (Figure 1b). The average size of $CoFe_2O_4$ nanoparticles was ca. 60 nm, and together with CNCs they formed a connected network on the support. The SEM−EDS (Figure 1c) and elemental analysis gave an Fe/Co ratio in the hybrids close to 2, in agreement with the initial reaction conditions.

To explore the organization of the CNCs and the CNC−$CoFe_2O_4$ dispersion at the oil/water interface we prepared emulsions containing hexadecane as the oil phase with oil/water ratio of 30/70 by weight. Neat CNCs have been reported to be efficient particle stabilizers for hexadecane-in-water emulsions, and therefore the same system was chosen here as a model.[3−5] It has been shown that the morphology as well as the surface properties affect how CNCs assemble at an emulsion interface.[5,36] In the case of the sulfated CNC the electrostatic repulsion between the particles can be reduced either by surface modification or by screening of the charges, both leading to interfacial destabilization. Here we used charge screening. The neat CNCs prior to modification with the inorganic particles successfully stabilized the hexadecane-in-water emulsion. The procedure used here led to formation of a system consisting of the emulsion phase residing on the top of the test tube and the excess water phase in the bottom, similarly to the many previous studies (see, for example, ref 3). Prior to the emulsion formation the CNCs were dyed with a fluorescent dye enabling observation of the emulsions with a confocal fluorescence microscope (Figure 2a). The emulsion was observed for one week, during which it was found to be stable. Some excess of the CNCs were noted to deposit in the aqueous phase as indicated by the coloration with calcofluor white stain, which was used as a fluorescent dye for the CNCs (see Supporting Information, Figure S3). This can be due to the electrostatic repulsion between the particles at low ionic strength.

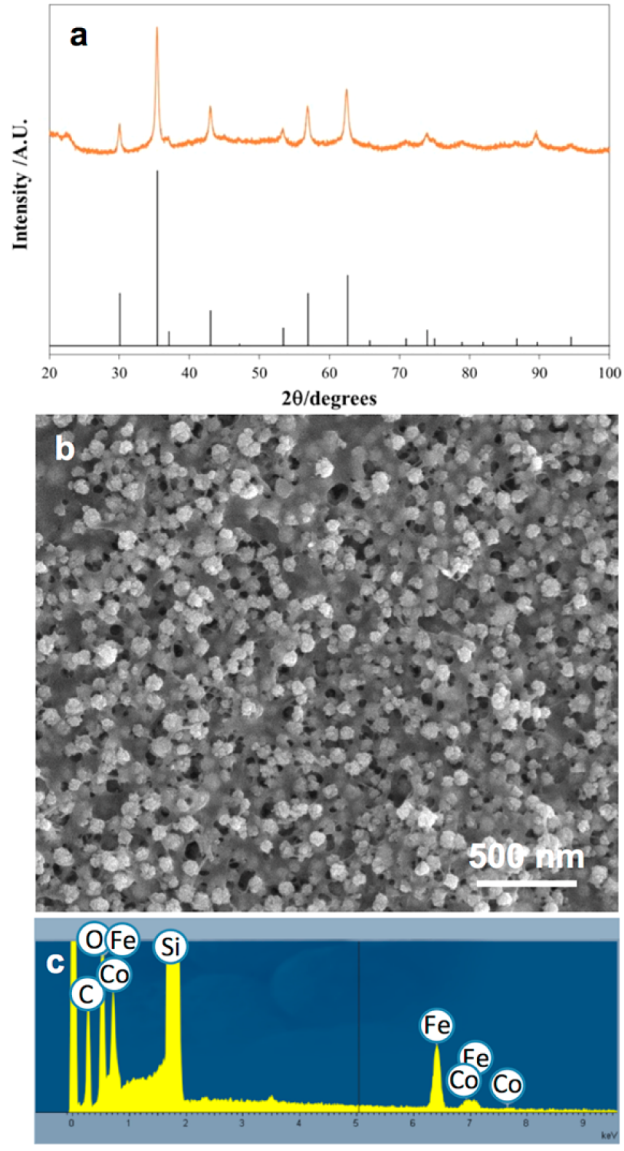

Figure 1. (a) XRD pattern of the CNC−$CoFe_2O_4$ hybrid (top). A reference $CoFe_2O_4$ pattern is shown on the bottom. (b) SEM image of $CoFe_2O_4$ nanoparticles coupled to CNC support forming a film. EDS spectrum of the CNC−$CoFe_2O_4$ material is shown in (c). The Si signal comes from the sample's substrate.

Also the CNC−$CoFe_2O_4$ aqueous dispersion was mixed with hexadecane, sonicated to emulsify the system, and was found to be equally effective for emulsion stabilization (Figure 2b). The average sizes of the Pickering emulsions stabilized by the neat CNC or the CNC hybrid shell were 8.4 ± 2.1 and 6.9 ± 1.7 μm, respectively. Hence, considering the standard deviation both emulsions contained droplets of similar size. Evidently the CNC hybrid shell has at least similar capability to assemble at the hexadecane/water interface as does the neat CNC shell, and clearly, the inorganic loading does not hinder the self-assembly. In fact, use of the CNC hybrid shell should be more effective for the Pickering stabilization considering that with the sulfated CNCs decreasing the electrostatic repulsion results in improved stability of the Pickering emulsions[36] and that in our previous work we reported a lower negative zeta potential value for the CNC−$CoFe_2O_4$ material than for the neat CNC.

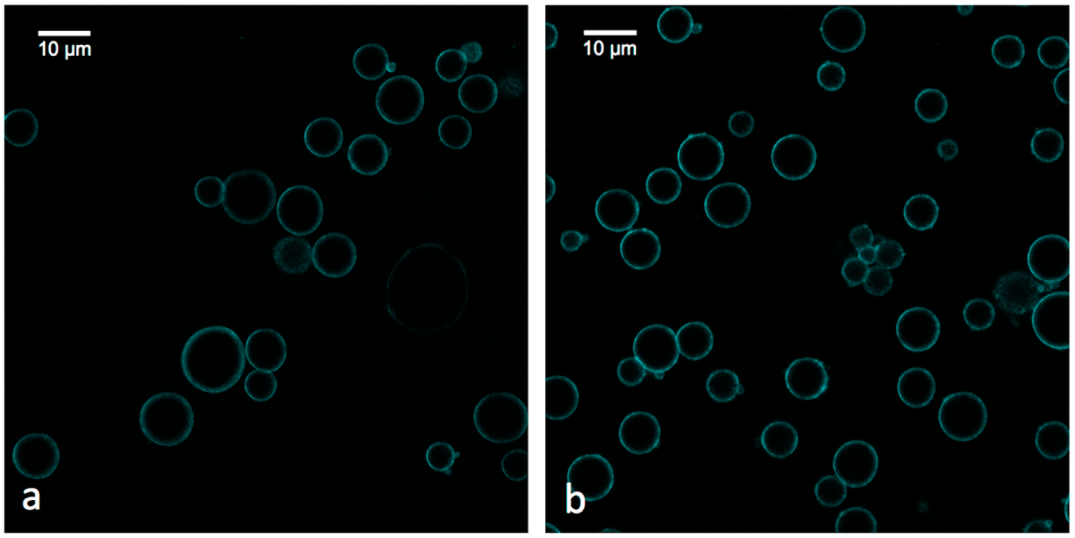

Figure 2. Confocal fluorescence microscope imaging of hexadecane-in-water emulsion stabilized by (a) neat CNCs and (b) CNC−$CoFe_2O_4$ shell. The stabilizing dispersions were dyed with Calcofluor white stain prior to emulsion preparation.

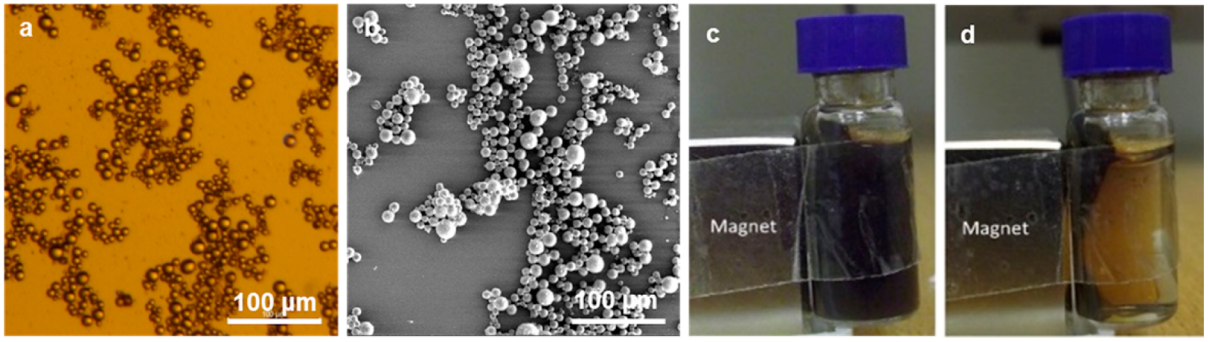

Figure 3. (a) Optical microscopy and (b) SEM images of polystyrene microbeads encapsulated by hybrid CNC−$CoFe_2O_4$ shells. The microbeads can be separated by magnetic manipulation as shown in (c, d).

The encapsulation of the oil droplets in shells formed by CNC−$CoFe_2O_4$ makes an excellent precursor system for solid bead formation. In addition to providing an emulsion system for preparation of microbeads encapsulated by a CNC hybrid shell, these findings suggest obvious potential of the CNC−$CoFe_2O_4$ material in preparation of stimuli-responsive emulsions for noncontact magnetic manipulation.

Styrene has also been reported to exhibit an ability to form emulsions with similar drop size and polydispersity as hexadecane.[36] Therefore, styrene-in-water Pickering emulsions stabilized by the magnetic CNC layer were used as a precursor for magnetic microbead preparation. The styrene-in-water Pickering emulsions with the CNC−$CoFe_2O_4$ hybrid particles at the droplet interface were formed with CNC concentrations as low as 4 wt % with respect to the styrene monomer. Additionally, a control experiment with the styrene-in-water emulsion was performed by preparing two emulsions, one with CNCs as a Pickering stabilizer and another with single neat ferrite particles (see images of the emulsions in the Supporting Information, Figure S4). Although there was adsorption of the neat ferrite particles on the interface (the particles are in the top oil-rich phase), it is clear that emulsions are much more uniform and stable with the CNC shell; the droplet size is also much larger for neat ferrite particles than for CNC as stabilizer.

The styrene core was exposed to initiator and elevated temperature leading to polymerization into PS. After polymerization of the styrene in the Pickering emulsions, PS microparticles encapsulated in the hybrid CNC−$CoFe_2O_4$ shells were obtained. As deduced from Figure 3a,b the average size of the microbeads was 8 μm (standard deviation $\pm$3 μm), which is significantly smaller than what is generally reported for polymer particles produced from Pickering emulsions stabilized with pure isotropic magnetic nanoparticles.[37−39] To our knowledge only one report exists for mixtures of isotropic and anisotropic magnetic nanomaterials for emulsions stabilization.[40] In this previous study carbon nanotubes with attached magnetite nanoparticles were used; however, the resultant droplets were much larger compared to the ones presented here. Clearly, the utilization of the CNCs enables formation of fairly small microbeads, whereas the spherical magnetic particles provide the magnetic functionality.

The resulting microbeads encapsulated with the CNC hybrid shell could be attracted by a magnet and separated from the media demonstrating their response to magnetic field (Figure 3c,d). The possibility of guiding the microbeads by magnetic manipulation suggests their potential for use in magnetic-field facilitated delivery of materials encapsulated in the CNC−$CoFe_2O_4$ shell. We are envisioning that the magnetically manipulative CNCs can be used for in situ encapsulation of substances in aqueous media. The ability to gain spatial control of the encapsulated structures under an applied magnetic field suggests that these substances can be removed, separated, or

delivered to/from different locations or media. The saturation magnetization of the magnetically separated CNC−$CoFe_2O_4$ was ca. 60 emu g^{-1}. For a detailed characterization of the magnetic properties the reader is guided to our prior publication on the matter.[35]

The magnetic hysteresis loop (Figure 4) was used to further quantify the ferromagnetic behavior of the PS microparticles

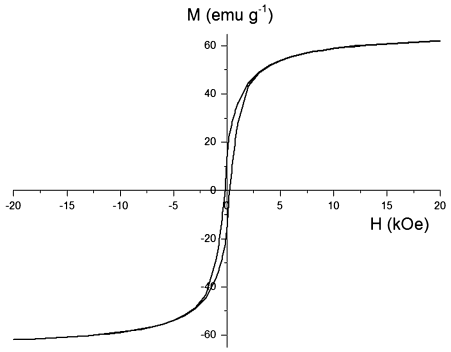

Figure 4. Magnetization curve of the dry hybrid microbeads at 298 K. Magnetization is expressed per gram of magnetic material.

encapsulated by the cellulose hybrid magnetic shell. The saturation magnetization (M_s) was 62 emu g^{-1} at 298 K, with a coercive field (H_C) of 0.3 kOe and a remanence (M_r) of 15 emu g^{-1}. The saturation magnetization and the remanence were lower than reported in a work where similar particles were synthesized in situ using a cellulose nanofibril network reporting values of ca. 74 and 47 emu g^{-1}, respectively.[41] However, the coercivity of the microbeads (23.9 kA m^{-1}) was close to the values of some of the samples studied by Galland et al.[41] The magnetization at saturation of the CNC−$CoFe_2O_4$ PS hybrid material was lower than that of bulk $CoFe_2O_4$ (80.8 emu g^{-1}) reported by Grigorova et al.[42] but higher than that of $CoFe_2O_4$ of smaller size prepared also by coprecipitation methods.[43,44] The larger size of nanoparticles in the present case also resulted in higher H_C and M_r values. Hence, clearly the magnetic moment of the particles is high enough to enable separation from the aqueous media as presented in Figure 3d.

SEM observations of the surface of PS microbeads revealed that they were coated by CNCs carrying $CoFe_2O_4$ nanoparticles (Figure 5). EDS analysis confirmed the presence of cobalt and iron in the microbeads (Figure S5 in the Supporting Information) and XRD analysis of the microbeads (Figure S6 in the Supporting Information) indicated that the $CoFe_2O_4$ phase was preserved after polymerization.

The CNC−ferrite hybrids appear to form an entangled mesh (Figure 5b,c) that consists of CNCs covering the surface of the PS droplets with the magnetic particles extending from the surface and forming a three-dimensional surface structure. Such a structure creates a hindrance between the droplets in the emulsion, which explains the effective stabilization. The in situ synthesis of the magnetic particles with CNCs[35] enables the particles to bind together, leading to the encapsulating mesh to be formed. A few submicron-sized PS particles were also observed on the surface of the larger PS microbeads (marked by arrows in Figure 5d), resulting from secondary nucleation outside the hybrid-coated droplets.

It is evident that utilization of hybrid CNCs in the formation of the microcapsules enables a surface-specific loading of the

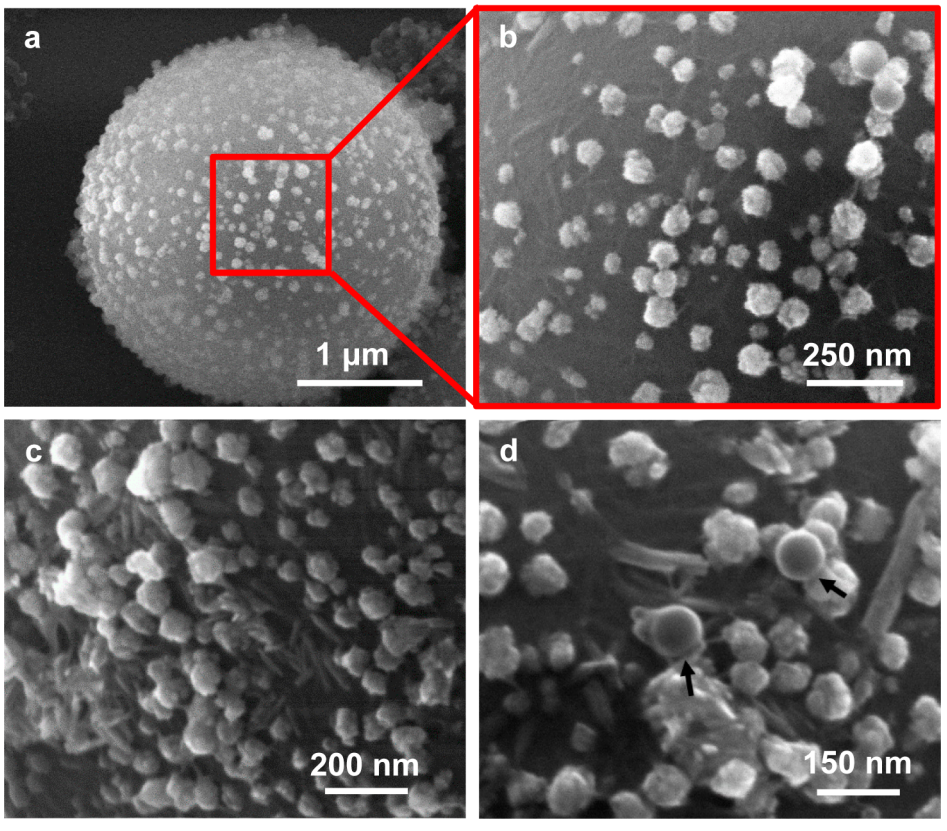

Figure 5. SEM images of (a) an individual hybrid CNC−$CoFe_2O_4$−PS microbead and (b, c) close-ups to the surface revealing the CNC hybrid mesh formation. Arrows in (d) indicate small PS particles formed by nucleation outside emulsion droplets.

ferrite particles, making the microcapsules magnetically responsive. Incorporating the magnetic functionality to the microbeads adds to the use of cellulose microspheres in separation in aqueous systems. The magnetic loading of the hybrid microbeads can be further increased if nanoparticles are also incorporated in the PS core. This is easily achieved by dispersing presynthesized, hydrophobized, magnetic nanoparticles in the monomer prior to the emulsification step. Our preliminary experiments have demonstrated that $CoFe_2O_4$ nanoparticles (ca. 15 nm) prepared by a hydrothermal method[45] can be loaded at concentrations as high as 20 wt % in the CNC-stabilized microbeads (see SEM images, EDS spectrum, and some details on ex situ $CoFe_2O_4$ nanoparticle synthesis in the Supporting Information, Figure S7).

The potential of the CNC−$CoFe_2O_4$ encapsulated microbeads for purification and separation was demonstrated in preliminary experiments by monitoring the concentration in aqueous solution of a cationic dye, methylene blue (Figure 6),

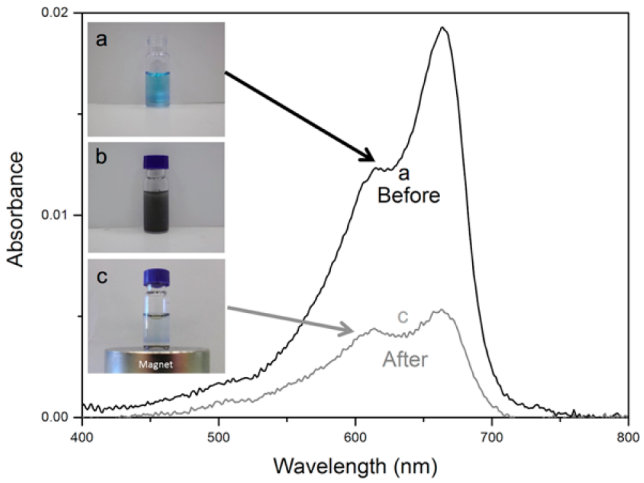

Figure 6. (a) Methylene blue removal from aqueous solution by introducing (b) CNC−cobalt ferrite PS hybrid microbeads to the solution. Methylene blue solution after magnetic separation of the dye saturated microbeads is shown in (c). UV−vis spectra of the methylene blue solution before (a) and after (c) adsorption are presented on the right.

which preferentially adsorbs on the surface of negatively charged CNCs.[34] Cationic dyes such as methylene blue have several undesirable effects on humans when released to wastewaters.[46,47] As presented by Wang et al.[48] new efficient methods for water purification in this area are needed, and utilization of magnetic cellulose microbeads are proposed here as a possible alternative. As shown in Figure 6 the CNC−$CoFe_2O_4$ encapsulated microbeads effectively removed methylene blue from solution (Figure 6a,b). The hybrid particles carrying the dye could be concentrated and separated from the media by a magnet (Figure 6c). Clearly, once an analyte or probe molecule is trapped by the beads, they can be concentrated or moved to different location or media. On the basis of the UV−vis analysis the adsorption of the dye in the conditions used was estimated to be ca. 2 mg g^{-1} of the microbeads.

The microbeads presented in Figure 5 were further used to prepare hollow microcapsules using the polymer matrix as a sacrificial template. Acetone added to the dispersion containing the microbeads induced strong aggregation but appeared to permeate through the hybrid CNC−ferrite shell, causing PS dissolution to yield hollow capsules (Figure 7a). This approach led to some intact or partially collapsed hollow microcapsules, with the CNC−$CoFe_2O_4$ shell remaining on the surface of the microcapsules (Figure 7b,c). These results are an indication that the CNC−$CoFe_2O_4$ mesh was strong enough to withstand the stress produced by dissolution of the PS core and preparation procedures used for imaging.

CONCLUSIONS

CNC−$CoFe_2O_4$ nanoparticle hybrids synthesized by coprecipitation were assembled at oil/water interface leading to formation of Pickering emulsions. These emulsions were subsequently used as templates for fabrication of magneto-responsive polymer microbeads with a hybrid CNC−$CoFe_2O_4$ shell. Uniform and strong attachment of metallic particles on the CNC phase was demonstrated. The CNC hybrid material was able to form a tightly packed mesh with magnetic functionality on the bead surface.

Utilizing a combination of CNCs with the in situ synthesized magnetic particles enabled a high magnetic response even at low loading. The prepared microbeads were smaller in size compared to other studies reporting on magnetic microbeads. Furthermore, hybrid CNC−$CoFe_2O_4$ hollow microcapsules could be produced by dissolution of the polymer core. The ability of the cellulose microbeads for dye removal from aqueous solutions, for example, as a model for wastewater decontamination, was demonstrated and suggests major potential in separation and purification applications. These findings open new possibilities for utilization of the magneto-

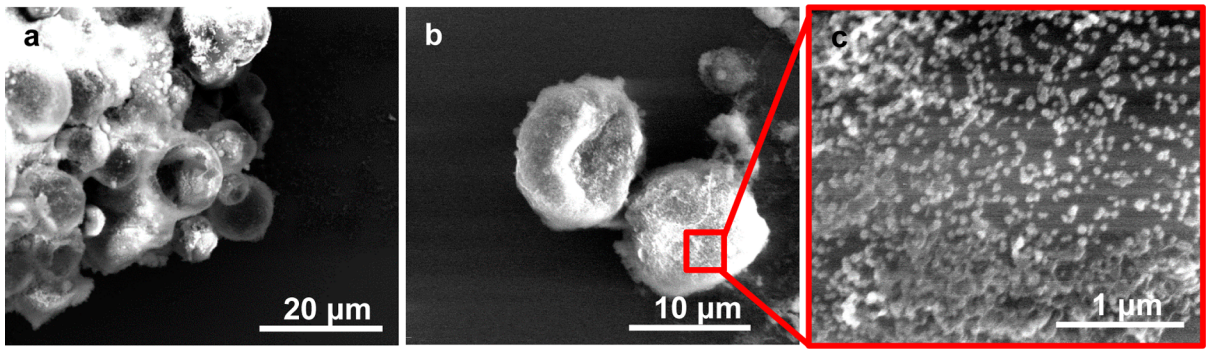

Figure 7. (a) SEM imaging of CNC−$CoFe_2O_4$ microcapsules prepared by dissolution of the PS core, (b) magnification of an individual capsule, and (c) a close-up to the capsule surface confirming presence of the CNC hybrid shell.

responsive CNC material for in situ capturing and separation from liquid media, in stimuli-responsive Pickering emulsions, and in preparation of functional cellulose microbeads.

■ ASSOCIATED CONTENT

Supporting Information

A figure presenting CNCs; TGA analysis of the CNC−$CoFe_2O_4$ particles; an image of hexadecane-in-water Pickering emulsion stabilized with the CNC−$CoFe_2O_4$ particles; images of the styrene-in-water emulsions formed using the CNC and neat ferrite particles; EDS spectrum of the PS microbeads covered with cellulose−ferrite nanoparticles; XRD pattern of the microbeads; images and EDS spectrum of CNC encapsulated PS microbeads with a neat CNC shell. This material is available free of charge via the Internet at http://pubs.acs.org.

■ AUTHOR INFORMATION

Corresponding Authors

*E-mail: tiina.nypeloe@boku.ac.at. (T.N.)
*E-mail: carlos.rodriguez@inl.int. (C.R.-A.)

Present Address

⊥Boku University of Natural Resources and Life Sciences Vienna, Konrad Lorenz Straße 24, 3430 Tulln an der Donau, Austria.

Author Contributions

The manuscript was written through contributions of all authors. All authors have given approval to the final version of the manuscript.

Notes

The authors declare no competing financial interest.

■ ACKNOWLEDGMENTS

T.N. acknowledges Emil Aaltonen Foundation for funding. C.R.-A. is grateful for funding from the European Union's Seventh Framework Program (FP7/2007-2013) under COOPERATION program NMP-theme, Grant No. 314212. O.R. acknowledges support by the Academy of Finland's Centres of Excellence Programme and HYBER (2014-2019). Dr. E. Johannes at Cellular and Molecular Imaging Facility at North Carolina State University is acknowledged for the confocal fluorescent microscope imaging.

■ REFERENCES

(1) Habibi, Y.; Lucia, L. A.; Rojas, O. J. Cellulose Nanocrystals: Chemistry, Self-Assembly, and Applications. *Chem. Rev.* **2010**, *110*, 3479−3500.

(2) Hanif, Z.; Ahmed, F. R.; Shin, S. W.; Kim, Y.; Um, S. H. Size-and Dose-Dependent Toxicity of Cellulose Nanocrystals (CNC) on Human Fibroblasts and Colon Adenocarcinoma. *Colloids Surf., B* **2014**, *119*, 162−165.

(3) Kalashnikova, I.; Bizot, H.; Cathala, B.; Capron, I. New Pickering Emulsions Stabilized by Bacterial Cellulose Nanocrystals. *Langmuir* **2011**, *27*, 7471−7479.

(4) Zoppe, J. O.; Venditti, R. A.; Rojas, O. J. Pickering Emulsions Stabilized by Cellulose Nanocrystals Grafted with Thermo-Responsive Polymer Brushes. *J. Colloid Interface Sci.* **2012**, *369*, 202−209.

(5) Kalashnikova, I.; Bizot, H.; Bertoncini, P.; Cathala, B.; Capron, I. Cellulosic Nanorods of various Aspect Ratios for Oil in Water Pickering Emulsions. *Soft Matter* **2013**, *9*, 952−959.

(6) Tasset, S.; Cathala, B.; Bizot, H.; Capron, I. Versatile Cellular Foams Derived from CNC-Stabilized Pickering Emulsions. *RSC Adv.* **2014**, *4*, 893−898.

(7) Wen, C.; Yuan, Q.; Liang, H.; Vriesekoop, F. Preparation and Stabilization of D-Limonene Pickering Emulsions by Cellulose Nanocrystals. *Carbohydr. Polym.* **2014**, *112*, 695−700.

(8) Sèbe, G.; Ham-Pichavant, F.; Pecastaings, G. Dispersibility and Emulsion-Stabilizing Effect of Cellulose Nanowhiskers Esterified by Vinyl Acetate and Vinyl Cinnamate. *Biomacromolecules* **2013**, *14*, 2937−2944.

(9) Pickering, S. U. Emulsions. *J. Chem. Soc., Trans.* **1907**, *91*, 2001−2021.

(10) Binks, B. P. Particles as Surfactants - Similarities and Differences. *Curr. Opin. Colloid Interface Sci.* **2002**, *7*, 21−41.

(11) Svagan, A. J.; Musyanovych, A.; Kappl, M.; Bernhardt, M.; Glasser, G.; Wohnhaas, C.; Berglund, L. A.; Risbo, J.; Landfester, K. Cellulose Nanofiber/Nanocrystal Reinforced Capsules: A Fast and Facile Approach Toward Assembly of Liquid-Core Capsules with High Mechanical Stability. *Biomacromolecules* **2014**, *15*, 1852−1859.

(12) Zhang, T.; Zhang, Q.; Chen, J.; Fang, K.; Dou, J.; Gu, N. The Controllable Preparation of Porous PLGA Microspheres by the Oil/Water Emulsion Method and its Application in 3D Culture of Ovarian Cancer Cells. *Colloids Surf., A* **2014**, *452*, 115−124.

(13) Yu, S.; Yao, Q.; Zhou, G.; Fu, S. Preparation of Hollow Core/Shell Microspheres of Hematite and its Adsorption Ability for Samarium. *ACS Appl. Mater. Interfaces* **2014**, *6*, 10556−10565.

(14) Phadke, K. V.; Manjeshwar, L. S.; Aminabhavi, T. M. Microspheres of Gelatin and Polyethylene Glycol Coated with Ethyl Cellulose for Controlled Release of Metronidazole. *Ind. Eng. Chem. Res.* **2014**, *53*, 6575−6584.

(15) Ettenauer, M.; Loth, F.; Thümmler, K.; Fischer, S.; Weber, V.; Falkenhagen, D. Characterization and Functionalization of Cellulose Microbeads for Extracorporeal Blood Purification. *Cellulose* **2011**, *18*, 1257−1263.

(16) Patchan, M. W.; Baird, L. M.; Rhim, Y.; LaBarre, E. D.; Maisano, A. J.; Deacon, R. M.; Xia, Z.; Benkoski, J. J. Liquid-Filled Metal Microcapsules. *ACS Appl. Mater. Interfaces* **2012**, *4*, 2406−2412.

(17) Zoppe, J. O.; Habibi, Y.; Rojas, O. J.; Venditti, R. A.; Johansson, L.; Efimenko, K.; Österberg, M.; Laine, J. Poly (N-Isopropylacrylamide) Brushes Grafted from Cellulose Nanocrystals Via Surface-Initiated Single-Electron Transfer Living Radical Polymerization. *Biomacromolecules* **2010**, *11*, 2683−2691.

(18) Csoka, L.; Hoeger, I. C.; Rojas, O. J.; Peszlen, I.; Pawlak, J. J.; Peralta, P. N. Piezoelectric Effect of Cellulose Nanocrystals Thin Films. *ACS Macro Lett.* **2012**, *1*, 867−870.

(19) Gutierrez, J.; Fernandes, S.; Mondragon, I.; Tercjak, A. Conductive Photoswitchable Vanadium Oxide Nanopaper Based on Bacterial Cellulose. *ChemSusChem* **2012**, *5*, 2323−2327.

(20) Kettunen, M.; Silvennoinen, R. J.; Houbenov, N.; Nykänen, A.; Ruokolainen, J.; Sainio, J.; Pore, V.; Kemell, M.; Ankerfors, M.; Lindström, T.; Ritala, M.; Ras, R. H. A.; Ikkala, O. Photoswitchable Superabsorbency Based on Nanocellulose Aerogels. *Adv. Funct. Mater.* **2011**, *21*, 510−517.

(21) Carrazana-Garcia, J. A.; Lopez-Quintela, M.; Rivas, J. Ferrimagnetic Paper Obtained by in Situ Synthesis of Substituted Ferrites. *IEEE Trans. Magn.* **1995**, *31*, 3126−3130.

(22) Carrazana-García, J. A.; Lopez-Quintela, M.; Rivas, J. Characterization of Ferrite Particles Synthesized in Presence of Cellulose Fibers. *Colloids Surf., A* **1997**, *121*, 61−66.

(23) Marchessault, R.; Rioux, P.; Raymond, L. Magnetic Cellulose Fibres and Paper: Preparation, Processing and Properties. *Polymer* **1992**, *33*, 4024−4028.

(24) Marchessault, R. H.; Ricard, S.; Rioux, P. In Situ Synthesis of Ferrites in Lignocellulosics. *Carbohydr. Res.* **1992**, *224*, 133−139.

(25) Raymond, L.; Revol, J.-F.; Marchessault, R. H.; Ryan, D. H. In Situ Synthesis of Ferrites in Ionic and Neutral Cellulose Gels. *Polymer* **1995**, *36*, 5035−5043.

(26) Wu, W. B.; Jing, Y.; Gong, M. R.; Zhou, X. F.; Dai, H. Q. Preparation and Properties of Magnetic Cellulose Fiber Composites. *BioResources* **2011**, *6*, 3396−3409.

(27) Olsson, R. T.; Azizi Samir, M. A. S.; Salazar-Alvarez, G.; Belova, L.; Ström, V.; Berglund, L. A.; Ikkala, O.; Nogues, J.; Gedde, U. W.

Making Flexible Magnetic Aerogels and Stiff Magnetic Nanopaper using Cellulose Nanofibrils as Templates. *Nat. Nanotechnol.* **2011**, *5*, 584−588.
(28) Sourty, E.; Ryan, D.; Marchessault, R. Ferrite-Loaded Membranes of Microfibrillar Bacterial Cellulose Prepared by in situ Precipitation. *Chem. Mater.* **1998**, *10*, 1755−1757.
(29) Li, Y.; Zhu, H.; Gu, H.; Dai, H.; Fang, Z.; Weadock, N. J.; Guo, Z.; Hu, L. Strong Transparent Magnetic Nanopaper Prepared by Immobilization of Fe_3O_4 Nanoparticles in a Nanofibrillated Cellulose Network. *J. Mater. Chem. A* **2013**, *1*, 15278−15283.
(30) Chen, L.; Berry, R. M.; Tam, K. C. Synthesis of B-Cyclodextrin Modified Cellulose Nanocrystals (CNCs)@ Fe_3O_4@ SiO_2 Superparamagnetic Nanorods. *ACS Sustainable Chem. Eng.* **2014**, *2*, 951−958.
(31) Mahmoud, K. A.; Lam, E.; Hrapovic, S.; Luong, J. H. Preparation of Well-Dispersed Gold/Magnetite Nanoparticles Embedded on Cellulose Nanocrystals for Efficient Immobilization of Papain Enzyme. *ACS Appl. Mater. Interfaces* **2013**, *5*, 4978−4985.
(32) Lam, S.; Blanco, E.; Smoukov, S. K.; Velikov, K. P.; Velev, O. D. Magnetically Responsive Pickering Foams. *J. Am. Chem. Soc.* **2011**, *133*, 13856−13859.
(33) Blanco, E.; Lam, S.; Smoukov, S. K.; Velikov, K. P.; Khan, S. A.; Velev, O. D. Stability and Viscoelasticity of Magneto-Pickering Foams. *Langmuir* **2013**, *29*, 10019−10027.
(34) Batmaz, R.; Mohammed, N.; Zaman, M.; Minhas, G.; Berry, R. M.; Tam, K. C. Cellulose Nanocrystals as Promising Adsorbents for the Removal of Cationic Dyes. *Cellulose* **2014**, *21*, 1655−1665.
(35) Nypelö, T.; Rodriguez-Abreu, C.; Rivas, J.; Dickey, M.; Rojas, O. J. Magneto-Responsive Hybrid Materials Based on Cellulose Nanocrystals. *Cellulose* **2014**, *21*, 2557−2566.
(36) Kalashnikova, I.; Bizot, H.; Cathala, B.; Capron, I. Modulation of Cellulose Nanocrystals Amphiphilic Properties to Stabilize Oil/Water Interface. *Biomacromolecules* **2012**, *13*, 267−275.
(37) Wang, C.; Zhang, C.; Li, Y.; Chen, Y.; Tong, Z. Facile Fabrication of Nanocomposite Microspheres with Polymer Cores and Magnetic Shells by Pickering Suspension Polymerization. *React. Funct. Polym.* **2009**, *69*, 750−754.
(38) Hasell, T.; Yang, J.; Wang, W.; Li, J.; Brown, P. D.; Poliakoff, M.; Lester, E.; Howdle, S. M. Preparation of Polymer−nanoparticle Composite Beads by a Nanoparticle-Stabilised Suspension Polymerisation. *J. Mater. Chem.* **2007**, *17*, 4382−4386.
(39) Kovalenko, A.; Jouhannaud, J.; Polavarapu, P.; Waton, G.; Pourroy, G. Hollow Magnetic Microspheres obtained by Nanoparticle Adsorption on Surfactant Stabilized Microbubbles. *Soft Matter* **2014**, *10*, 5147−5156.
(40) Wang, H.; Lin, K.; Jing, B.; Krylova, G.; Sigmon, G. E.; McGinn, P.; Zhu, Y.; Na, C. Removal of Oil Droplets from Contaminated Water using Magnetic Carbon Nanotubes. *Water Res.* **2013**, *47*, 4198−4205.
(41) Galland, S.; Andersson, R. L.; Salajková, M.; Ström, V.; Olsson, R. T.; Berglund, L. A. Cellulose Nanofibers Decorated with Magnetic Nanoparticles−synthesis, Structure and use in Magnetized High Toughness Membranes for a Prototype Loudspeaker. *J. Mater. Chem. C* **2013**, *1*, 7963−7972.
(42) Grigorova, M.; Blythe, H.; Blaskov, V.; Rusanov, V.; Petkov, V.; Masheva, V.; Nihtianova, D.; Martinez, L. M.; Munoz, J.; Mikhov, M. Magnetic Properties and Mössbauer Spectra of Nanosized $CoFe_2O_4$ Powders. *J. Magn. Magn. Mater.* **1998**, *183*, 163−172.
(43) Ayyappan, S.; Philip, J.; Raj, B. Effect of Digestion Time on Size and Magnetic Properties of Spinel $CoFe_2O_4$ Nanoparticles. *J. Phys. Chem. C* **2008**, *113*, 590−596.
(44) Sharifi, I.; Shokrollahi, H.; Doroodmand, M. M.; Safi, R. Magnetic and Structural Studies on $CoFe_2O_4$ nanoparticles Synthesized by Co-Precipitation, Normal Micelles and Reverse Micelles Methods. *J. Magn. Magn. Mater.* **2012**, *324*, 1854−1861.
(45) Kolen'ko, Yu. V.; Bañobre-López, M.; Rodríguez-Abreu, C.; Carbó-Argibay, E.; Sailsman, A.; Piñeiro-Redondo, Y.; Cerqueira, M. F.; Petrovykh, D. Y.; Kovnir, K.; Lebedev, O. I. Large-Scale Synthesis of Colloidal Fe_3O_4 Nanoparticles Exhibiting High Heating Efficiency in Magnetic Hyperthermia. *J. Phys. Chem. C* **2014**, *118*, 8691−8701.
(46) Garg, V.; Amita, M.; Kumar, R.; Gupta, R. Basic Dye (Methylene Blue) Removal from Simulated Wastewater by Adsorption using Indian Rosewood Sawdust: A Timber Industry Waste. *Dyes Pigm.* **2004**, *63*, 243−250.
(47) Rafatullah, M.; Sulaiman, O.; Hashim, R.; Ahmad, A. Adsorption of Methylene Blue on Low-Cost Adsorbents: A Review. *J. Hazard. Mater.* **2010**, *177*, 70−80.
(48) Wang, Y.; Zhang, X.; He, X.; Zhang, W.; Zhang, X.; Lu, C. In Situ Synthesis of MnO_2 Coated Cellulose Nanofibers Hybrid for Effective Removal of Methylene Blue. *Carbohydr. Polym.* **2014**, *110*, 302−308.